UDK 669.14.018.298:539.42
Izvirni znanstveni članek

ISSN 1580-2949
MTAEC9, 37(6)317(2003)

ON THE CHARPY FRACTURING PROCESS

O PROCESU CHARPYJEVEGA PRELOMA

Franc Vodopivec, Boris Arzenšek, Dimitrij Kmetič, Jelena Vojvodič-Tuma

Institute of Metals and Technology, Lepi pot 11, 1000 Ljubljana, Slovenia
franc.vodopivec@imt.si

Prejem rokopisa – received: 2003-06-16; sprejem za objavo – accepted for publication: 2003-11-10

The Charpy fracturing process was investigated for two structural steels. The relationships of load versus deflection and time were recorded from the upper to lower shelf temperature and the time and the deformation relative to different fracturing events were assessed. The consumption of energy for different fracturing events, as f.i. elastic and plastic deflection and crack propagation was deduced. The size of the plastic zone and the stress concentration at the notch tip were also deduced. A specific fracture micromorphology was observed in a thin layer of the fracture surface ahead the notch tip.

Key words: Load-deflection, time dependences, time to crack initiation and to fracture, elastic and plastic deformation, energy for different Charpy fracturing events, crack initiation, fracture surface micromorphology.

Raziskan je bil Charpyjev prelomni proces pri dveh konstrukcijskih jeklih. Izmerjene so bile odvisnosti sila-upogibek in sila-čas za območje temperature od zgornjega do spodnjega praga žilavosti in določena sta bila čas in deformacija pri različnih dogodkih prelomnega procesa. Določena je bila poraba energije za različne dogodke preloma, npr. elastični in plastični upogibek ter širjenje razpoke. Velikost plastične zone in koncentracija napetosti ob konici zareze sta bili tudi določeni. Posebna oblika prelomne površine je bila opažena v tanki plasti ob konici zareze.

Ključne besede: odvisnost sila-upogibek, čas do začetka razpoke, elastična in plastična deformacija, energija različnih dogodkov Charpyjevega preloma, začetek razpoke, mikromorfologija prelomne površine.

1 INTRODUCTION

Charpy (CVN) toughness tests are videly used to determine the effect of temperature on the propensity of structural steels to brittle fracture. Notched specimens are submitted to the impact of a hammer with the kinetic energy of 300 J. The fracturing occurs in ductile, mixed or brittle mode and, accordingly, a very different quantity of energy is consumed. Generally, in the upper shelf CVN ductile region, the energy consumed for the fracture of structural steels is 150 J and more and it is different for different steels. For the same steel the energy consumed for the brittle cleavage fracture below the lower shelf threshold is around 10 J and very similar for steels with different microstructure, a wide range of grain size and yield stress as well as for as delivered and strain aged steels (**Figure 1**). The fracturing time depends on the fracturing energy and it is very different, it is of 11 ms with the energy of 250 J and of 1 ms with the energy of 11 J. Also the volume of the plastically deformed metal is very different, it amounts to several hundreds of mm^3 in the ductile range and it is negligeble and below 1 mm^3 in the brittle range.

Virtually 90 % of the energy consumed for the plastic deformation and the ductile fracturing is transformed to heat[2,29]. For this reason, the fracturing in the upper shelf and transition range occurs significantly above the nominal testing temperature[3]. In brittle range virtually no heat is generated with plastic deformation and the fracturing occurs at the nominal testing temperature. Therefore, this temperature, which is currently used to show graphically the dependence CVN toughness versus testing temperature, does not represent the real fracturing temperature for the vhole testing interval. This fact should be considered when establishing correlations between the tensile properties and the CVN value in upper shelf and in transition temperature range. The fact that the fracturing temperature differs from the nominal the more, the greater is the CVN value entangles additionally the understanding of the CVN fracturing mechanism.

Let us quote some opinions on the different events involved in the CVN fracturing process. It is stated[4] that the Charpy tests consists of a variety of cumulative events and that several events in the fracturing zone are competitive in terms of local stress and strain. The Charpy specimen is to small to develop a steady state fracture mode[5]. The sensitivity to brittle fracture depends on the size of the tip radius[6]. It is assumed that the cleavage fracture is initiated with a ductile mode propagating crack when the tensile stress exceeds a critical stress on a certain microstructurally determined distance ahead the crack tip[7]. Britlle fracturing is initiated on carbide or/and nonmetallic particles ahead the crack tip[8]. The change from ductile to brittle crack propagation mode occurs after plastic slip ahead the ductile crack tip[9,10] and the critical COD and crack tip radius size were calculated for the fracture mode change[11]. The energy absorbed for the fracture depends on the amount of plastic deformation prior to crack initiation and multiple activation of crack sources takes place[12]. Mixed mode fracture energy is increased by a

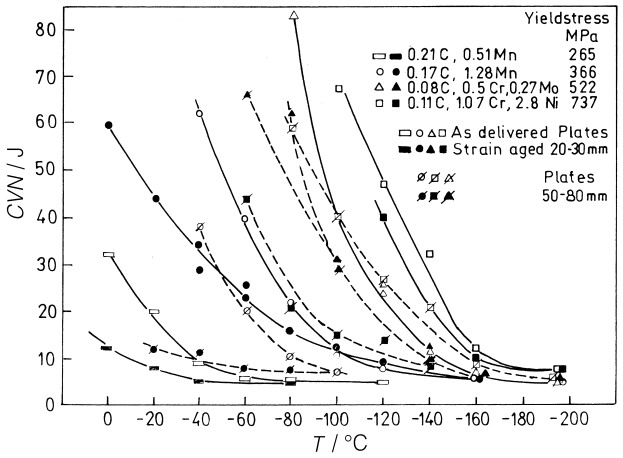

Figure 1: Charpy notch toughness for structural steels with different mikrostrukture and yield stress both sides the lower threshold notch toughness[1]

Slika 1: Charpyjeva zarezna žilavost za konstrukcijska jekla z različno mikrostrukturo in mejo plastičnosti na obeh straneh spodnjega praga žilavosti

factor of two as the crack inclination angle is decreased from 90° to 60° toward the specimen axis by tests at liquid nitrogen temperature, while at room temperature this angle has no effect on the fracture energy[13]. The combined criterion for cleavage fracture consists of a critical plastic strain for the initiation of the crack nucleus, a critical stress triaxiality for preventing its blunting and a critical normal stress for its propagation[14]. By reducing the notch tip radius on a CVN specimen, the stress concentration at the crack tip is increased[15]. Three caracteristic points: the yield, the maximal stress and the inflection and the areas of energy consumed up to the maximal load, energy consumed from this point to the inflection are found on the Charpy load versus time signal[16]. On brittle fracture river patters are found on (110) cleavage facets, while the (100) facets are smooth[17]. The cleavage fracture strength is a temperature[18,19] and grain size[20,21] dependent steel property.

These short quotations from the very selected references shows that some events of the Charpy fracturing process are well understood, while the fracturing process, as the joining of these events was not yet explained. In this article the results of tests performed with the aim to determine a comprehensive explanation of the follow up of the Charpy fracturing events are presented and discussed.

2 EXPERIMENTAL WORK

The tests were performed on two structural steels with the composition in **Table 1** steel A with a microstructure of polygonal ferrite and pearlite and intercept grain size of 35 μm and steel B with a microstructure of quenched and tempered ferrite and pearlite with the intercept grain size of 3.47 μm. Both steels were earlier used in the investigations on properties of as delivered and strain aged steels with yield stress from 265 to 1000 MPa and the microstructure of ferrite and pearlite and tempered martensite[22,23]. Tests with standard CVN specimens were performed on an instrumented Charpy hammer with computer recording of the load (deflection force) and the specimen deflection and loading time. Two parallel tests were performed for every temperature in the range from the upper to the lower shelf notch toughness. As shown in **Figure 2** this range was sligthly different for both steels. From the load force versus deformation and versus fracturing time relationships different data relative to the fracturing events were acquired. All fractures were visually examined and some of them also investigated with SE microscopy.

The load (deflection force) and deflection were measured in time intervals of 10 μs. In **Figure 3** three typical dependences fracturing force versus deflection and testing time for different CVN levels and fracturing

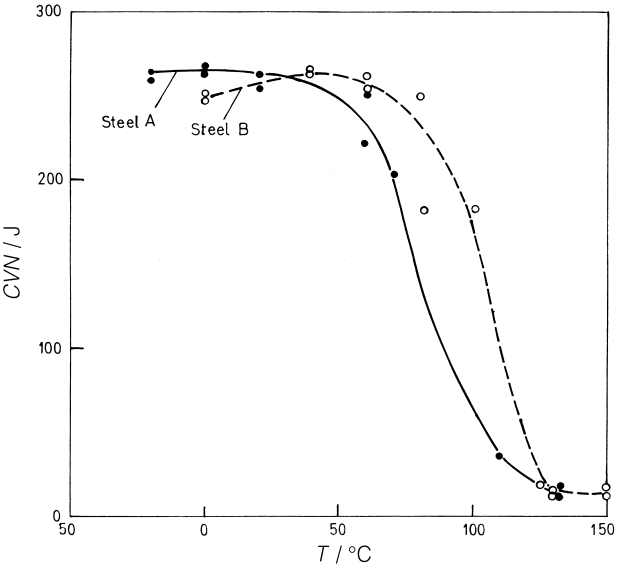

Figure 2: Effect of testing temperature on notch toughness (*CVN*) for the investigated steels A and B

Slika 2: Vpliv temperature preizkusa na zarezno žilavost (*CVN*) jekel A in B

Table 1: Composition of the investigated steels
Tabela 1: Sestava preiskovanega jekla

Steel	The mass fraction of elements (%)										
	C	Si	Mn	P	S	Cr	Ni	Mo	Nb	Al	N
A	0.17	0.32	1.28	0.02	0.01	0.21	0.13	–	–	0.045	0.009
B	0.08	0.34	0.36	0.01	0.004	0.54	0.27	0.27	0.058	0.052	0.007

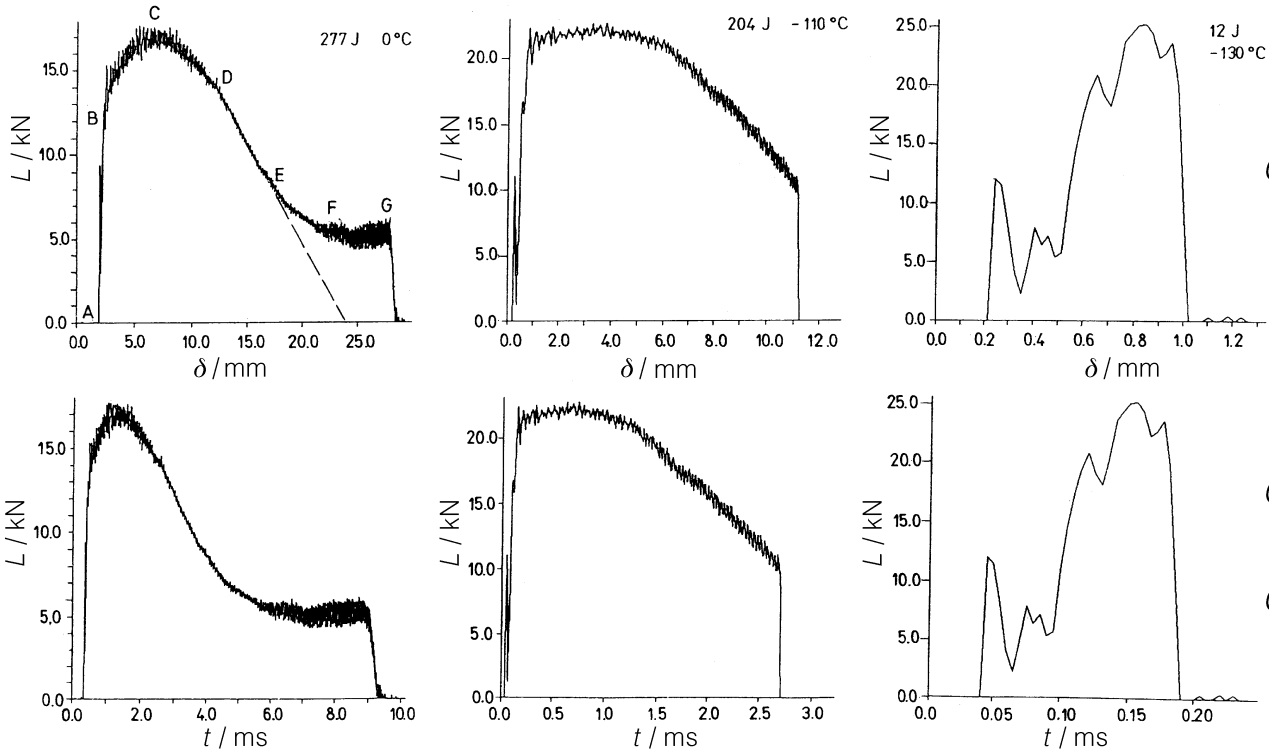

Figure 3: Steel A. Recorded load-deflection and load-time curves for different test temperature and *CVN* level
Slika 3: Jeklo A. Odvisnost sila-upogibek in sila-čas za različne temperature in žilavosti

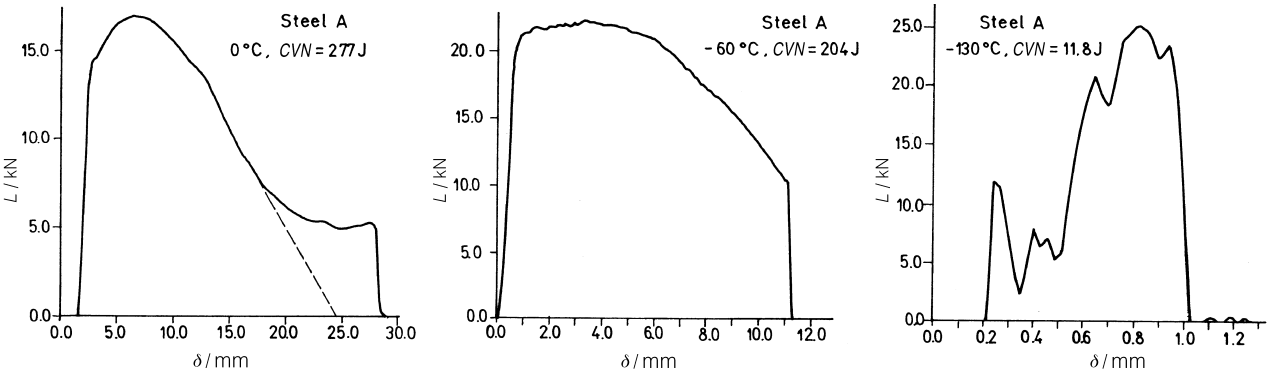

Figure 4: Steel A. Smoothened load-deflection (*L*-*δ*) curves for different temperature and *CVN* levels
Slika 4: Jeklo A. Glajene odvisnosti sila-upogibek (*L*-*δ*) za različne temperature in žilavosti

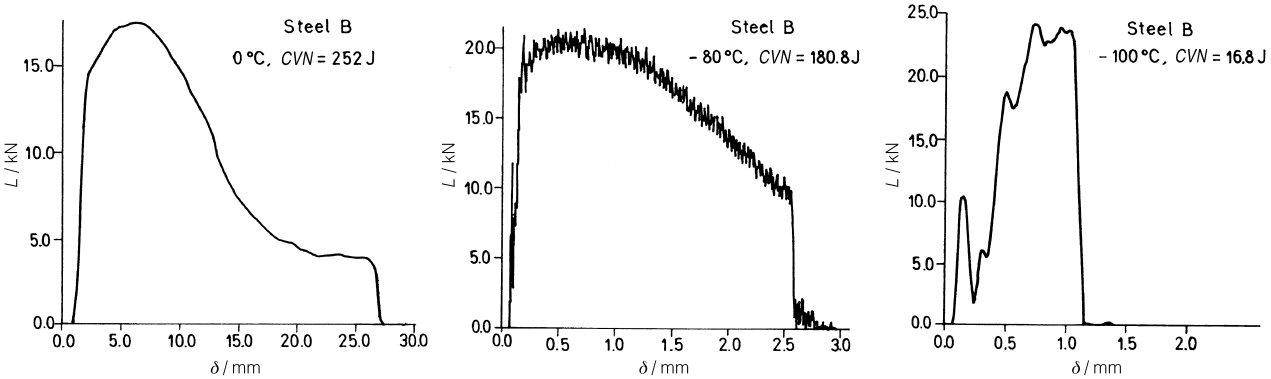

Figure 5: Steel B. Smoothened load-deflection (*L*-*δ*) curves for different temperature and *CVN* levels
Slika 5: Jeklo B. Glajene odvisnosti sila-upogibek (*L*-*δ*) za različne temperature in žilavosti

processes are shown. One or more load peacs due the elastic rebounding of the couple specime+hammer from the specimen supports precede the true increase of the deflection force. The rebounding amplitude was up to 12 kN, the duration up to 50 μs, the recoil up to 0.3 mm and the energy consumed up to 2 % by great CVN value with ductile fracture. A similar rebounding was reported for Charpy tests on heat treated steels[24]. In the following text dependences load versus deflection (L-δ curves) will be used, which were obtained with linear smoothening of the curves in figure 3 over time interval of 10 μs. Olthough details were probably lost in the smoothening, the smoothed curves allow a reliable identification of deformation and fracturing events occuring with the CVN test. Both, load versus deflection and load versus time curves are of equal shape.

3 DEPENDENCE LOAD VERSUS DEFLECTION

In **Figures 4 and 5** some dependences load versus specimen deflection (L-δ curve) are shown for both steels in the range from the upper to the lower shelf temperature. From the upper to the lower shelf range the fracturing energy and time are decreased more than one order of magnitude. Depending on the energy consumed for the fracturing events for both steels the three typical shapes of L-δ curves in **Figures 4 and 5** are distinguished.

For the highest fracturing energy (curve I) the load increases proportionally to the deflection up to the point B, where plastic strain is started. The deflection force increases than up to the maximum at the point C. Of side this point the load decreases first in non linear way with increasing deflection to the point D. Afterwards, it continues to decrease appr. proportionally to the deflection down to the inflection point E. Beyound this point the deflection starts to increase faster and behind point F it continues to increase by virtually constant load to drop to zero at the point G. In the A to B range the specimen is bend elastically and the load increases proportionally to the deflection. In the range B to C plastic deformation of the specimen occurs and the load (L) increases parabolically to the deflection (δ), thus $L = k + f(\delta)^{1/2}$, with δ as deflection, as shown in **Figure 6**.

The crack (fracture) is started at the point of maximal load C[16]. Visual examination showed several cracks initials in the notch by ductile and brittle fracturing, as reported allready[11,14]. On the side surface of some specimens it was evident that the propagation was arrested for the cracks which propagated outside the notch plane of maximal stress. No evidence of parallel crack initiation was found on the L-δ curves. It is concluded that the initiation of all cracks on the specimen was virtually simultaneus. Of-side the point C the non linear C-D part of the L-δ curve is approximately symmetrical to the B-C on-side part and the deflection force does not decrease proportionally to the crack length. This indicates to the continuation of strain hardening over the remaining ligament of the specimen. At the point D, where the fracture has propagated for appr. 2.5 mm, the load start to decrease appr. proportionally to the increasing deflection and without further increase of strain hardening down to the point E.

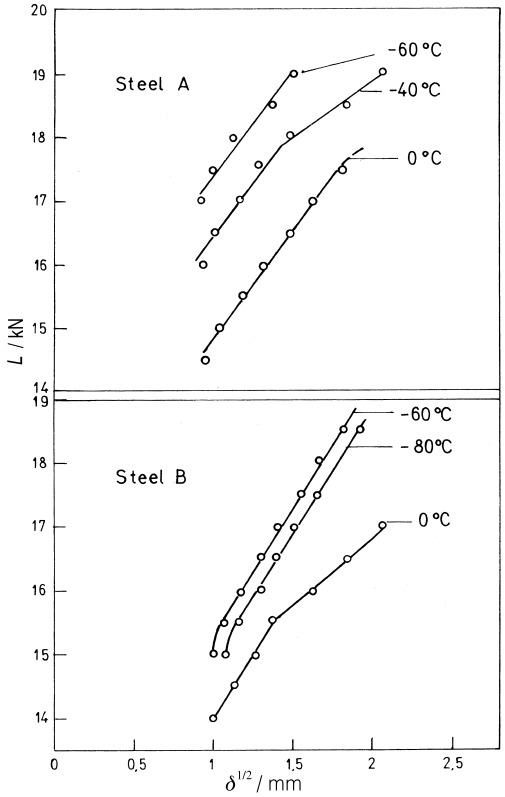

Figure 6: Load-deflection dependence in the B to C part of some L-δ curves
Slika 6: Jeklo B. Odvisnost sila-upogibek za B do C del nekaterih odvisnosti L-δ

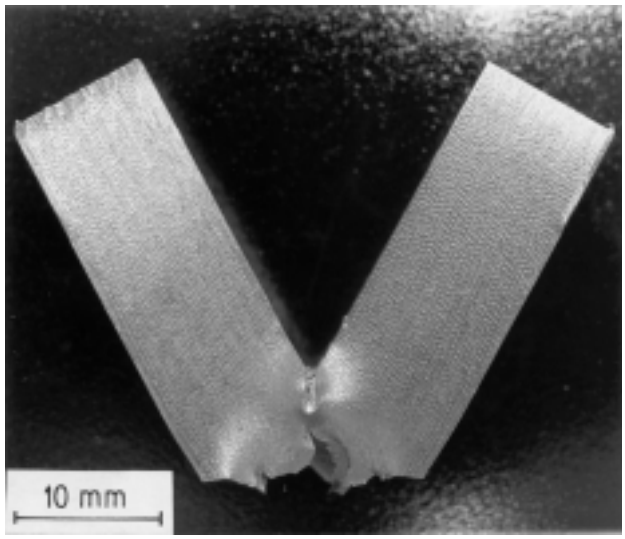

Figure 7: Shape of one specimen with L-δ curve I after ejection
Slika 7: Oblika preizkušanca z odvisnostjo I L-δ po izmetu

Since the plastic deformation is continued and the great majority of plastic strain energy is transformed to heat[2] it is assumed that in this part of the *L-δ* curve the temperature in the metal ahead the propagating crack is increased to a level of significant decrease of the steel strength. The rapid increase of the deflection of side the point E is due to the thrusting of the specimen in the gap between its supports, which occurs in the part F-G of the *L-δ* curve without further crack propagation. At the point E the angle between the actual and the initial position of the specimen was of about 45° and the deflection of 13.5 to 14.5 mm. Beyound the point F and at the deflection of 21 mm to 22 mm the specimen is bent to the maximum and it is finally ejected at the point G with the shape shown in **Figure 7**. The energy consumed in the F to G part of the *L-δ* curve does not represent a part of the true steel fracturing energy. In absence of specimen thrusting the fracturing would continue as shown by the dashed prolongation of the linear part D-E in **Figure 3-I**.

The energy consumed for the thrusting of the unbroken specimen through the gap amounted to 5.3 J to 21 J rsp. 2 % to 7.6 % of the total ductile fracturing energy in the upper shelf region. Sheaves of parallel low steps in the area of maximal lateral striction on the side surface of specimens with the highest CVN energy (**Figure 8**) show that the plastic deformation is not uniform and that over small areas single stress components of triaxiality predominates.

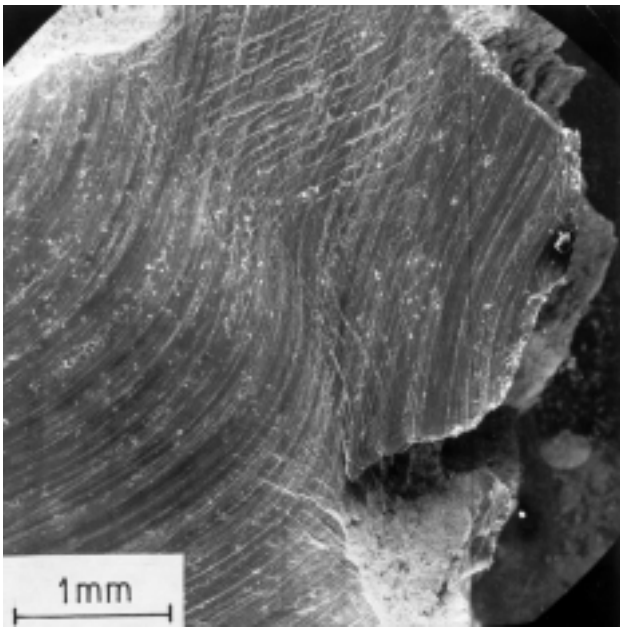

Figure 8: Curved machining scratches and sheaves of short and straight deformation steps in the area of maximal lateral striction on the side surface of the specimen in **Figure 7**

Slika 8: Ukrivljene obdelovalne raze in snopi kratkih ravnih deformacijskih stopnic na bočni površini v območju največje lateralne kontrakcije preizkušanca na **sliki 7**

By intermediate value of notch toughness and at a temperature inside the transition range, (curve II in **Figures 4 ad 5**), the plastic deformation starts at the point B at higher load on account of the increased yield stress. Beyound the point B the load increase to the point C with a lower rate and extent of strain hardening as in the *L-δ* curve I. Of side the pont D, where the fracture has propagated for appr. 2.5 mm, the load decreases proportionally to the deflection down to the point E, where the abrupt fracturing occurs with transgranular cleavage. At this point the angle of the bent specimen to the initial position is of about 30° and the fracture has propagated for appr. 4,7 mm over the section of the specimen. Also on specimens with *L-δ* II curve several cracks were found to start in the notch tip and became unpropagating after sufficient deviation from the notch plane.

The dependence III in **Figures 4** and **5** was recorded on specimen fractured in the lower shelf range. The stress amplitude of the initial rebounding was up to 12 kN, the time up to 50 μs, the recoil up to 0.25 mm and the fracture time of appr. 1 ms. It is not possible to ascertain if all the initial peacs are due to the elastic rebounding or some may represent the formation of a secondary crack and its arrest after deviation outside the notch plane. The actual fracture is represented by the on-side part in the *L-δ* curve with the maximal load. While a significant part of the total CVN energy was consumed also for the elastic rebounding, it is not possible to detemine the energy consumed eventually for the apperance and the propagation of secondary cracks. The fracture occurred with the total deflection of appr. 1 mm and the specimen angle of 2° with respect to its initial position.

4 PARAMETERS OF *L-δ* DEPENDENCES LOAD AND SPECIMEN FRACTURING TIME

From the *L-δ* curves the following parameters were selected as significant for the different events of the fracturing process: the fracture rate and time, the elastic deflection and the deflection at the maximal load where the fracturing process was started. The different deflections were determined reliably only on the *L-δ* curves I and part of them on *L-δ* curves II.

The fracturing events consume different shares of CVN energy. The shares of elastic energy and energy consumed for the specimen drag can be determined reliaby, while the share of plastic deformation energy can be determined realiably only for the B to C part of the *L-δ* curve. Off side the point C and up to point D the energy is spent for both, the plastic deformation and the crack propagation. In the part D to E of the *L-δ* curves of the type I the energy is consumed only for the fracturing process and it decreases parallely to the decrease of the ligament section.

The stress termed Charpy yield stress (R_{EC}) and the theoretical elastic deflection (δ_t) were calculated considering the deflection force and the deflection at the point B assuming that the specimen was an unnotched beam with the central neutral axis and the linear distribution of stresses over the section using the relations:

$$R_{EC} = L\ l\ h/8\ I = 3\ F\ l/a\ h^2 \quad \text{and} \quad \delta_t = Ll^3/48\ E\ I \qquad (1)$$

With: L – load (deflection force), l – distance between the specimen supports (l = 40 mm), I – moment of inertia ($I = bh^3/12$) with b- and h- width and height of the specimen in the notch plane) and E – elastic modulus.

The factor of stress concentration as measure of the index of triaxiality, is calculated from the relation[25]

$$K_p = 1 + \ln(1 + R/r) \qquad (2)$$

And the radius of the plastic zone ahead the crack tip from the relation[26]

$$r = \rho\ \{\exp[(R_C/R_E) - 1] - 1\} \qquad (3)$$

Where R is the size of the plastic zone, r is the notch tip radius, R_C is the clevage strength, R_E is the yield stress in uniaxial tension and ρ is the notch tip radius.

According to[27] the cleavage fracture in a low alloyed bainitic A508 Class II steel is largerly independent of the temperature above appr. –160 °C. The cleavage strength increases in a coarse grained polygonal ferrite and pearlite steel with lower temperature due to the increase in lower yield stress[28] and the difference

$$\Delta\sigma = R_C - R_E \qquad (4)$$

is nearly constant. For the investigated steel A by tensile test of notched specimens at –120 °C the cleavage strength R_c = 1250 MPa was determined for a yield stress R_E = 480 MPa[11]. In this case the difference is $\Delta\sigma$ = 770 MPa. The load at the start of plastic deformation in the L-δ curves in **Figures 1 and 2** represents the actual stress at the crack tip (R_{EC}). The ratio of this stress versus the yield stress in uniaxial tensions (R_E) represents in first approximation the stress concentration factor, thus $K_p = R_{EC}/R_E$. Using this ratio and the radius of the notch of Charpy specimens ρ = 0.2 mm it is possible to deduce the size of the plastic zone (R) ahead the notch.

In **Table 2** the values for the Charpy yield stress, for the Charpy strength determined from the L-δ curves, the theoretical elastic deflections calculated according to the equation (1), the experimentally determined elastic deflections and the size of the plastic zone calculated from equations (2) and (3) are given for different temperature and both investigated steels.The Charpy yield stress and the Charpy strength increase with the lowering temperature and are greather by the steel with higher yield stress. The theoretical elastic deflection increases slightly with decreasing temperature and it is greater for the steel B with higher yield stress. The experimental elastic deflection, determined as deflection at the end of the initial linear part of L-δ curves I and II, is constant down to –60 °C. It is smaller at lower temperature when the shape of the L-δ curve changes from mode I to mode II and it is similar in both investigated steels. The ratio $K_p = CR_E/R_E$ is independent on temperature and it is greater for the steel A with lower yield stress. The size of the plastic zone calculated from relation (3) is greater for the steel A. It increases slightly with decreasing temperature and it is smaller for the L-δ curve II.

Table 2: Data on the Charpy fracturing process
Tabela 2: Podatki o procesu Charpyjevega preloma

Temp. °C	R_{EC} MPa	R_C MPa	δ mm	$\delta_{exp.}$ mm	R_1 mm	R_2 mm	K_p	δ_{ci} mm	(L-δ) curve
Steel A									
60	1105	1713	0.34	0.63				4.9	I
20	1168	1828	0.35	0.62	1.76	1.48	3.22	5.0	I
0	1190	1863	0.36	0.64	1.70	1.43	3.24	5.0	I
–20	1264	1897	0.38	0.66	1.88	1.35	3.36	5.1	I
–60	1540	2087	0.46	0.43	1.64	0.87	3.35		II
Steel B									
0	1259	1686	0.38	0.66	0.62	-	2.42	4.9	I
–40	1391	1802	0.42	0.68	0.82	-	2.63	5.0	I
–60	1405	1823	0.42	0.69	0.80	-	2.62	5.1	I
–80	1423	1972	0.43	0.41	0.74	-	2.54	3,2	II
–100	1494	1990	0.45	0.41	0.76	-	2.57	3.1	II

R_{EC} – Charpy yield stress, R_C – Charpy strength, δ_c – calculated elastic deflection, δ_{exp} – experimental elastic deflection, R_1 – size of the plastic zone according to eq. (3), R_2 – size of the plastic zone according to eq. (4), K_p – ratio Charpy yield stress versus uniaxial yield stress, δ_{ci} – deflection at maximal load and fracture initiation, (L-δ) – shape of the curve load versus deflection

The difference between the Charpy yield stress and the uniaxial yield stress reflects the triaxiality of stresses at the notch tip and the constraint effect. For the calculation of the theoretical elastic deflection the actual Charpy yield stress was considered and, suprisingly, the measured deflection is significantly greater. For the L-δ curves of shape II the measured elastic deflections are smaller and they agree acceptably with the deduced values. Very similar values obtained on several specimens show this finding to be reliable. It seems like the constraint effect and the stress triaxiality in the notch were reflected also in the elastic behaviour of the steels.

The difference in plastic zone size and in the index of triaxiality of both steels is due to the difference in yield stress. The plastic zone size calculated using two different methods agrees acceptably.

The brittle mode propagation is started when the plastic zone size (a) and its radius (ρ) have decreased to a critical value. For a steel of the same type as steel A a = 22 μm and ρ = 0.062 μm were deduced[11]. On the base of the force, the flexion and the crack length at the point E of the L-δ curves of the type II could be, on principle, used to determine the dinamic fracture toughness for the case of mixed mode of fracture propagation.

5 CONSUMPTION OF ENERGY FOR THE FRACTURING EVENTS

From the *L*-δ curves like those in **Figures 4 and 5** the energy consumed for the different events of the Charpy fracturing was determined: elastic and plastic deflection, crack initiation, crack propagation and thrusting the specimen through the gap as well as the time to crack initiation and to total fracture. The data are given in **Table 3**.

The average share of energy consumed for the elastic deflection amounts by steel A to 2.3 % and to 2.8 % in steel B. For the plastic deflection (deformation) before the crack initiation on average 28.1 % of the total energy was consumed for the steel A and 29.5 % for the steel B. The range of values obtained for specimens which the *L*-δ curve I and II is of 26,6 % to 31.8 % for the steel A and 27.3 % to 32.4 % for the steel B. In the limits of the experimental error for both steels, the plastic strain energy is independent on the total energy and on the test temperature. The total energy consumed up to the crack initiation is independent on the temperature. It amounts on average to 30.7 % of the total energy for the steel A and to 31.8 % for the stee B.

Approximately 2/3 of the total energy is consumed in the fracturing process after the crack was started. From *L*-δ curves I experimental values from 61.4 % to 70.3 % were established for the steel A and 61.4 % to 70.3 % for the stel B.

The linear decrease of the resistance to fracture propagation betwen points D and E on *L*-δ curves I is explained by the absence of additional strain hardening over the specimen ligament, which could be expected if the steel temperature was increased sufficiently. The fracturing proces is fast and it can be assumed that the heat generated by the plastic deformation is dissipated for 90 % as adiabatic heat[2,29] in the volume of metal, where the plastic deformation occurrs before and during the fracturing. The approximate increase of temperature above the nominal (ΔT/°C) in this layer of steel can deduced from the fracturing energy (*CVN*/J) using the relation:

$$\Delta T \approx 0.90\ (CVN)/\ v\ c\ p \qquad (5)$$

With v – volume of the deformed layer of steel, c – specific heat of the steel (c = 44,8 J/N °C) and p – density of the steel ($p = 7.86 \cdot 10^4$ N/m^3).

The consumption of energy in approximately 2 ms between the points D and E of the *L*-δ curve I is of CVN 49.6 J/ms. Between the points D and E the crack has propagated from a_D = 2.35 to a_E = 5 mm and the ligament area has decreased from $A_D = 5.65 \cdot 8 = 45.2$ mm^2 to

Table 3: Share of energy for different fracturing events
Tabela 3: Delež energije pri različnih lomnih dogodkih

Steel	Temp. °C	El. def.		Pl.def.		Cr. in.		Sp. dr.		Cr. pr.		Cr. in	(*L*-δ)
		J	%	J	%	J	%	J	%	J	%	ms.	curve
A	60	5.4	2.1	80.3	31.8	85.7	33.9	5.7	2.3	160.4	63.6	1.1	I
		6.2	2.6	73.3	28.9	79.5	31.5	5.6	2.2	160.5	63.2	1.0	I
	20	5.9	2.2	71.5	26.9	77.4	29.1	5.3	2.0	183.1	68.8	1.0	I
		5.7	2.2	79.9	30.0	85.6	30.3	5.9	2.2	172.3	65.2	1.0	I
	0	6.3	2.3	73.8	26.6	80.1	28.9	19.8	7.1	182.9	66.0	1.0	I
		6.0	2.2	79.1	28.8	85.1	31.0	21.1	7.6	169.6	61.4	1.1	I
	–20	6.1	2.4	71.6	28.0	77.7	30.4	16.7	6.5	160.4	62,9	1.0	I
		6.2	2.4	60.4	23.1	66.6	25.5	10.9	4.2	183.5	70.3	0.9	I
	–60	5.3	2.6	60.2	29.5	65.7	32.1	-	-	138.1	67.9	0.6	II
	–110	-	-	-	-	17.4	48.6	-	-	18.4	51.4	0.2	III
	–130	-	-	-	-	6.6	37.0	-	-	11.2	63.0	0.2	III
B	0	6.0	2.4	68.7	28.3	74.7	29.7	18.0	7.1	159.0	63.1	0.9	I
		6.1	2.5	70.3	28.5	76.4	31.0	18.6	7.5	151.8	61.4	1.0	I
	–40	6.6	2.6	76.9	29.9	83.5	32.5	17.6	6.8	155.6	60.5	1.0	I
		6.6	2.6	74.2	29.1	80.8	31.7	19.7	7.7	154.3	60.5	1.0	I
	–60	7.1	2.8	75.0	29.6	84.1	32.4	18.6	7.3	151.8	59.7	0.9	I
		7.2	2.7	72.8	27.8	80.0	30.5	16.9	6.5	164.8	62.9	1.0	I
	–80	4.1	2.3	58.4	32.4	62.5	34.7	-	-	117.3	65.3	0.7	II
		4.0	2.2	50.9	27.8	54.9	30.0	-	-	127.9	70.0	0.7	II
	–100	-	-	-	-	8.5	50.6	-	-	8.3	49.4	0.1	III
		-	-	-	-	8.9	82.4	-	-	1.9	17.6	0.1	III
	–130	-	-	-	-	7.6	64.4	-	-	4.2	35.6	0.1	III
		-	-	-	-	8.8	63.7	-	-	5.0	36.3	0.1	III

El. def. – elastic deflection, Pl. def. – plastic deflection, Cr. in. – deflection at maximal load and crack initiation, Sp. dr.- drag of the specimen in the gap through the supports, Cr. pr. – crack propagation, Cr. in. – time to crack initiation, (*L*-δ) – shape of the load deflection curve

$A_C = 2.96 \cdot 8 = 23.7$ mm^2. Considering an average ligament area of $A = 34.4$ mm^2 the following increases of temperature are deduced for the steel in deformation layers of thickness 3mm, 2 mm, 1 mm and 0.5 mm:136 °C, 204 °C mm, 408 °C and 816 °C. Theoretically, the generated temperature is sufficient to induce the steel recovery, which would explain the linear shape od the L-δ curve between the points D and E. The generated heat is rapidly dissipated in a volume of steel of complex shape, for that reason no marks of higher temperature are found on the fracture surface.

For L-δ III curves it is not possible to determine the elastic flexion of the specimen before the crack was initiated. This flexion and its consumption of energy are smaller with L-δ curves II than with L-δ curves I. It is assumed, that the energy consumed before the crack was started was below 4 J in case of L-δ curves III.

With the L-δ curves I part of energy was consumed for the thrust of the specimen between the supports. With the steel A this share of energy amounts to appr. 2.2 % of the total energy at 20 °C. It is much higher up to 7,6 % at 0 °C and lower. It is also greater with the steel B. The difference is greater than that expected from the difference in yield stress.

In the range of experimental error the time to crack initiation is identical with L-δ curves I and II. The plastic deformation starts after appr. 1 ms and the crack is opened appr. 5 ms after the contact of the hammer and the specimen. The time to fracture for the L-δ curves I was of 11 ms, of 2 to 3 ms for curves II and from 0.15 to 0.40 ms for curves III.

6 FRACTURE MICROMORPHOLOGY

The fracture surface of specimens tested in ductile range showed symmetrical dimples in areas of predominant effect of stress normal to the fracture plane and asymmetrical dimples in areas of stronger effect of shear stress. On most specimens tested in ductile range in a layer of width of approximately 50 μm (**Figure 9**) ahead the notch tip the fracture surface was flat with a rounded up ruggedness and small asymmetrical hollows and dimples, both on the scale of μm (**Figure 10**). It is asumed that this layer represents to the stretched layer at the crack initiation quoted in reference[12]. The rare dimples have the charateristic plastic ligament only in the directions parallel and orthogonal to the crack propagation. The transition from this layer to the asymmetrical dimpled area covering most of the fracture surface, was generally abrupt with microbulges evolving to asymmetrical fully formed dimples (**Figure 11**). The abrupt transition was occasionally interrupted with tongue shaped penetrations in the dimpled area (**Figure 12**). Great incomplete dimples with a botton similar to that in the surface layer and without ligament in the side direction of crack propagation were found also in the area of asymetrical dimples (**figure 13**). No marks of cleavage are found in the layer of fracture at the notch tip and it is assumed that it represents the fracturing with plane shearing with a minor effect of the tensile component of the triaxiality or the initial shear due to the slightly asimetric hammer stroke.

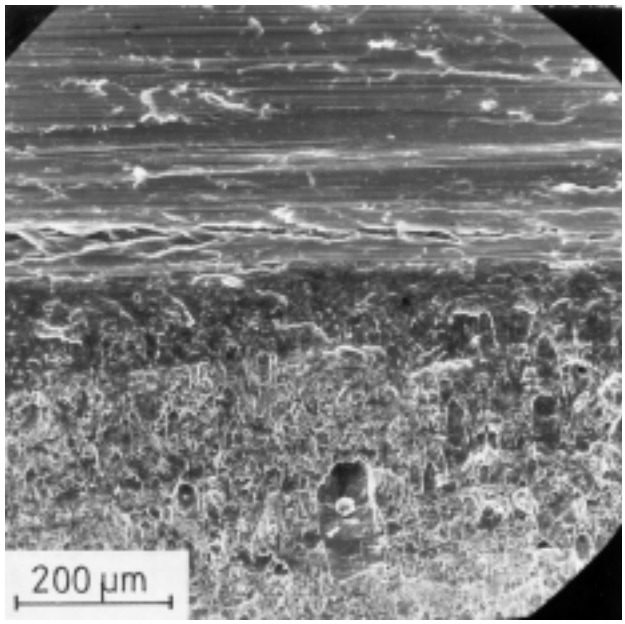

Figure 9: Steel A tested at 20 °C. Upper part: notch surface, intermediate layer without dimples and dimpled fracture on the lower part of the microfractography

Slika 9: Jeklo A, preizkus pri 20 °C. Zgornji del: površina zareze, vmesna plast brez jamic in jamičasta površina preloma na spodnjem delu posnetka

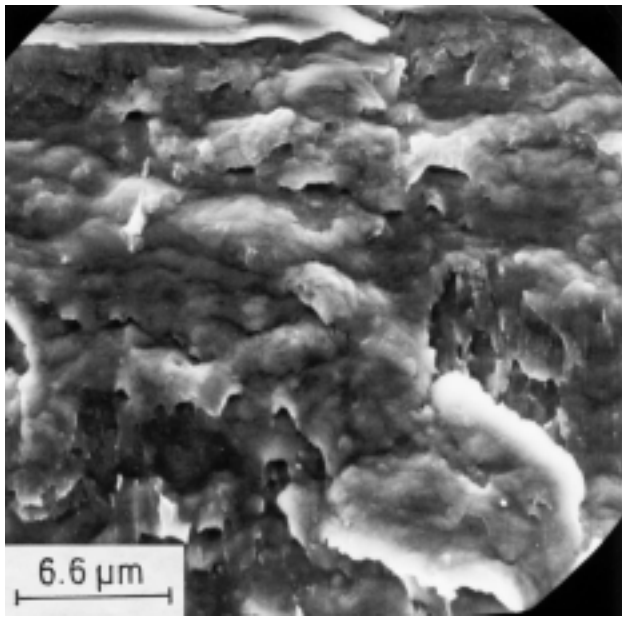

Figure 10: Specimen on **Figure 9**. Surface of the fracture layer at the crack tip

Slika 10: Preizkušanec na **sliki 9**. Površina preloma ob konici zareze

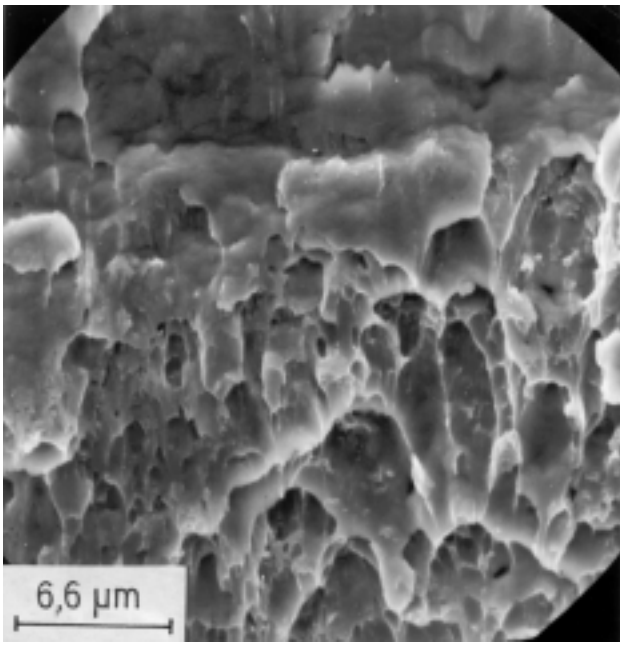

Figure 11: Specimen as in **Figure 9**. Transition from the area shown in **figure 9** to the area of fracture with asimetrical dimples
Slika 11: Preizkušanec na **sliki 9**. Prehod s površine na **sliki 9** v področje preloma z asimetričnimi jamicami

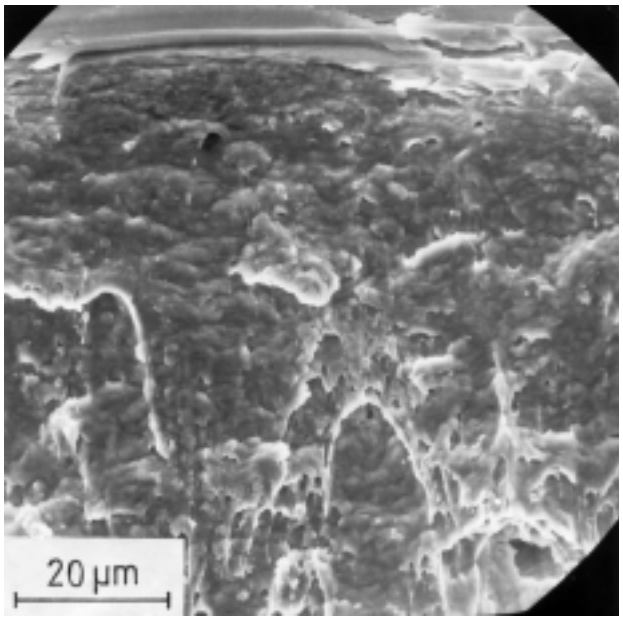

Figure 12: Detail from the right side of **Figure 9**. Tongue shaped penetrations from the intermediate layer in the dimpled area of the fracture surface
Slika 12: Detajl z desne strani **slike 9**. Jezičkasti prodori iz vmesne plasti v jamičasto prelomno površino

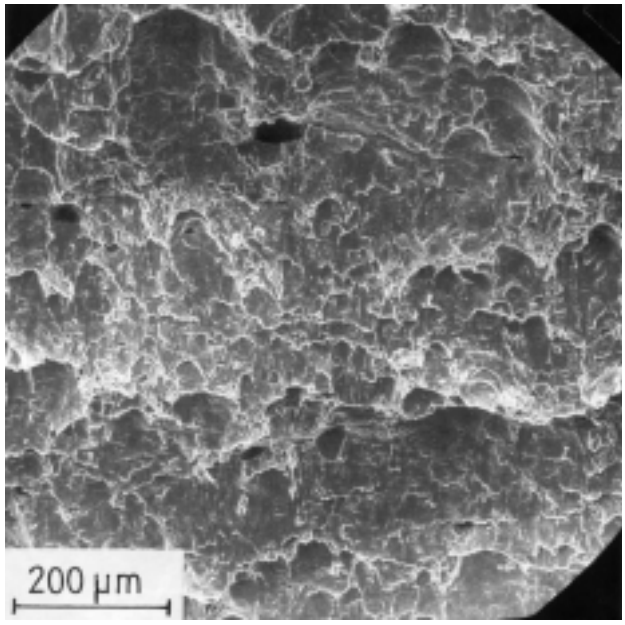

Figure 13: Mixed fracture surface morphology in the central part of specimen in **Figure 9**
Slika 13: Mešana površina preloma v srednjem delu preizkušanca na **sliki 9**

7 CONCLUSIONS

Notch toughness tests were carried out with two structural steels with different microstructure and yield stress in the temperature range from the upper shelf to the lower shelf Charpy toughness. The tests were performed on an instrumented Charpy device with load and deflection measured in intervals of 10 µs. The fracture surface was examined with scanning electron microscopy. Considering the results and conclusion in a number of quoted references as well as on the base of the presented results and their analysis the following conclusions are proposed:

I) Several events: elastic and plastic bending deformation, strain hardening, crack initiation and ductile crack propagation, adiabatic transformation of plastic strain energy to heat are interconnected in the fracturing process in the upper shelf range. The same events occurr in the transition range where also the abrupt change from ductile to brittle crack propagation occurrs on part of the specimen section. Of side the lower shelf range only elastic deformation and brittle crack propagation occurr.

II) The load versus deflection curve depends on the mechanism of crack propagation over the specimen section. The time to fracture in the interval from 1 to 11 ms depends also on the crack propagation mode.

III) Up to 2% of the total Charpy energy is consumed for the elastic rebounding of the specimen+hammer of the specimen supports. The rebounding load is up to 12 MN and the rebounding time is up to 150 µs.

IV) Several crack are initiated at the notch tip and are stopped if propagating outside the notch plane of maximal stress.

V) With ductile fracture a thin layer of ductile propagation virtually without dimples was found at the crack tip. With difference to the majority of the fracture surface, the micromorphology in this layer suggests a

propagation in conditions of triaxial stressing with a minor effect of the stress component normal to the fracture surface.

VI) Assuming that the Charpy specimens is a straight beam with a central neutral axis and a linear stress distribution over the section the ratio Charpy to uniaxial yield stress amounts to 3.25 ± 0.2 for the steel with a microstructure of polygonal ferrite and pearlite and to 2.5 ± 0.2 for the steel with a microstructure of quenched ferrite and pearlite and higher yield stress. The size of the plastic zone at the crack tip was of 1.42 mm for ductile and of 0.87 mm for mixed mode fracture of the steel 1. The flexion of the specimen at the crack opening in upper toughness is of (5 ± 0.2) mm for both steels. It is smaller with the mixed mode fracture.

VII) In the range of ductile and mixed fracture up to 2.5 % of the total energy is consumed for the elastic flexion of the specimen. With ductile fracturing (29.5 ± 3) % is consumed for the plastic deformation and (65.5 ± 5) % for the crack propagation events.

For the steel with the microstructure of polygonal ferrite and pearlite (2.1 ± 0.3) % of energy is consumed in the thrusting of the partially fractured specimenn between the supports. With the higher yield stress steel the thrusting consumes (6 ± 1.5) % of the total Charpy energy.

8 REFERENCES

[1] F. Vodopivec, J. Vojvodič-Tuma, Proc. Of the Int. Symposium Mechanical Properties of Advanced Engineering Materials, 27-31 mai 2001, Mie Un. Japan

[2] W. Dahl, H. Rees: Grundlagen des Festigkeits und Bruchverhalten, Verlag Stahleisen, 54-70, 1974, Düsseldorf

[3] F. Vodopivec, B. Breskvar, J. Vojvodič-Tuma, D. Kmetič: Kovine Zlitine Tehnologije (Metals Alloys Technology), 33 (**1999**) 393-400

[4] J. Lerein, J. D. Embury: Conf. Proc. What the Charpy tests show us, Dnever, CO, 27-28 nov. 1978, 33-53, Mater. Park, OH, ASM International

[5] G. M. Wilkowski, W. A. Maxey, R. J. Eiber: Ibidem 108-132

[6] C. E. Harbower, R. D. Sumbury: Ibidem, 151-171

[7] T. Miyata, A. Otsuka, M. Mitsubayashi, T. Haze, S. Aihara: Fracture Mechanics 21th Symposium, ASTM, Philad., STP 1074, 1990, 361-377

[8] J. F. Knott: J. Iron Steel Inst., 204 (**1966**) 104

[9] D. A. Curry: Met. Sci., 14 (**1980**) 319-326

[10] P. Brozzo, M. Capurro, E. Stagno: Mater. Sci. Technol., 10 (**1994**) 334

[11] F. Vodopivec, B, Breskvar, B. Arzenšek, D. Kmetič, J. Vojvodič-Tuma: Mater. Sci. Techn., 17 (**2001**) 1-7

[12] M. Naguno, Y. Sawano: J. Japan Inst. Metals, 54 (**1990**) 420-426

[13] B. H. J. Koch, C. A. Kwa, M. Manoharan: Inter. J. Fracture, 77 (**1996**) R77-R81

[14] J. H. Chen, G. Z. Wang, C. Yan, H. Ma, L. Zhu: Inter. J. Fracture, 83 (**1997**) 121-138

[15] S. Mikalac, M. G. Vassilaros, H. C. Rogers: Int. Conf. Charpy Impact Tests: Factors and Variables, Lake Buena Vista FLO, 1990, ASTM STP 1072, Phil., 134-141

[16] D. Pachura: 16th Intern. Conf. On Effects of Radiation on Materials, 23-25 june 1992, Aurora, CO, ASTM STP 1175 (**1994**) 195-210

[17] S. T. Mandziej: Metall. Trans. A, 24 A (**1993**) 545-552

[18] C. Jüde-Esser, F. Grimpe, W. Dahl: Steel Res., 66 (**1995**) 259-263

[19] D. A. Curry, J. F. Knott: Met. Sci., 10 (**1976**) 1-6

[20] D. A. Curry: Met. Sci., 14 (**1980**) 319-326

[21] R. Sandström, Y. Bergsström: Met. Sci., 18 (**1984**) 177-186

[22] F. Vodopivec, J. Vojvodič-Tuma, M. Lovrečič-Saražin: Metalurgija, 38 (**1999**) 127-137

[23] F. Vodopivec, J. Vojvodič-Tuma, M. Lovrečič-Saražin: Kovine Zlitine Tehnologije, 32 (**1998**) 463-470

[24] Đ. Dobi: Kovine Zlitine Tehnologije, 26 (**1992**) 63-73

[25] H. Kurishita, H. Nayano, M. Narui, M. Yamazaki, Y. Kano, I. Shibahara: Mater. Trans., JIM, 34 (**1993**) 1042-1052

[26] R. O. Ritchie, J. F. Knott, J. R. Rice: J. Mechan. Ohys. Solids, 21 (**1973**) 395-410

[27] D. A. Curry: Metals Sci., 16 (**1982**) 435440

[28] J. F. Knott: Trans. ISIJ, 21 (**1981**) 305-317

[29] R. J. Hand, S. R. Foster, C. M. Sellars: Mat. Sci. Techn. 16 (**2000**) 442